



# Magnetically thiamine palladium complex nanocomposites as an effective recyclable catalyst for facile sonochemical cross coupling reaction

Hossein Naeimi | Fatemeh Kiani

Department of Organic Chemistry,  
Faculty of Chemistry, University of  
Kashan, Kashan 87317, I.R., Iran

## Correspondence

Hossein Naeimi, Department of Organic  
Chemistry, Faculty of Chemistry,  
University of Kashan, Kashan 87317,  
I.R., Iran.  
Email: naeimi@kashanu.ac.ir

## Funding information

University of Kashan, Grant/Award  
Number: 159148/78

The carbon–carbon cross coupling reactions through transition-metal-catalyzed processes has been significantly developed for their important synthetic applications. In this research, we have shown that  $\text{NiFe}_2\text{O}_4@\text{TASDA-Pd}(0)$  is a highly active, novel and reusable catalyst with excellent performance for the Mizoroki–Heck coupling reaction of several types of iodo, bromo, and even aryl chlorides in DMF under ultrasound irradiation. The novel palladium catalyst prepared and characterized by using FT-IR spectrum, X-ray diffraction (XRD), scanning electron microscopy (SEM), Energy-dispersive X-ray spectroscopy (EDX), thermo gravimetric analysis (TGA) and vibrating sample magnetometer (VSM). The catalyst can be recovered and recycled several times without marked loss of activity.

## KEYWORDS

heterogenous catalyst, Mizoroki–heck reaction,  $\text{NiFe}_2\text{O}_4$ , Pd, ultrasound irradiation

## 1 | INTRODUCTION

Olefination of aryl halides, generally called the Heck cross coupling reaction,<sup>[1–3]</sup> which first time was investigated in 1971 has become a great and powerful tool for the formation of useful trans-stilbene derivatives.<sup>[4,5]</sup> The Mizoroki–Heck coupling reaction is one of the most widely used palladium-catalyzed C–C cross coupling reactions in modern organic synthesis, preparation of advanced enantioselective natural products and biologically active molecules, polymerization processes, production of pharmaceuticals, hydrocarbons, agrochemical and fine chemicals.<sup>[6–14]</sup> Many researchers investigated effective role of solvents during their studies on C–C cross coupling reactions.<sup>[15–19]</sup> Dipolar aprotic solvents such as dimethyl sulfide, acetonitrile, dimethyl formamide and N-methyl pyrrolidone are common solvents applied in the coupling reaction. Improvement of coupling reaction is highly dependent on the reactivity of the palladium catalyst. Commonly, catalysts are separated into two categories:

homogeneous systems and heterogeneous systems. Although the reported useful effects with homogeneous system, problems associated with the separation and recyclability of the expensive catalyst, limit their use in synthetic and industrial applications. Therefore, it is necessary to develop supported catalysts that can quickly be recycled from the reaction system and reused. Thus, in order to overcome these drawbacks, many researches on developing effective procedures for Pd complexes on several different solid supports, such as clays<sup>[20]</sup> activated carbon,<sup>[21]</sup> micro porous polymers,<sup>[22]</sup> and magnetic nanoparticles have been performed. Currently, magnetic feature provides a fantastic approach for separating magnetic nanoparticles with an external magnet. Magnetic nanoparticle supported catalysts are the best case as they not only show considerable catalytic activities but the magnetic nature of these particles also allows for facile recycling of the catalyst without use of the classical separation method.<sup>[23,24]</sup>

With the expanding environmental knowledge in chemical reaction, the challenge of designing stable

environmentally friendly methods has become the principal aim of green chemistry. From the first research on using ultrasound in organic reactions,<sup>[25]</sup> the tendency to use this tool in organic transformations developed greatly. Acoustic cavitation is a physical effects that assists organic synthesis under ultrasound irradiation. This phenomenon consists the formation, growth, and implosive collapse of bubbles in a solution during a short range of time. Precipitate implosion of these bubbles in the solution; create localized hot spots with short life times. The hot spot has a tantamount temperature of 5000 °C and pressure of about 2000 atmospheres. These transient, localized hot spots leading to a turbulent flow in the solution and enhanced mass transfer.<sup>[26,27]</sup> Therefore, in this, we focus on synthesis, full characterization and application of NiFe<sub>2</sub>O<sub>4</sub>@TASDA-Pd(0) complex which appears to be highly active recyclable catalyst for the Heck cross coupling reaction of styrene with various aryl halides.

## 2 | EXPERIMENT

### 2.1 | Materials and apparatus

All commercially available reagents were used without further purification and purchased from the Merck Chemical Company in high purity. The used solvents were purified by standard procedure.

The IR spectra were obtained as KBr pellets in the range of 400–4000 cm<sup>-1</sup> on a Perkin-Elmer 781 spectrophotometer. For recorded the <sup>1</sup>H NMR spectra we used Bruker (400 MHz) DRX-400 spectrometer in pure deuterated CDCl<sub>3</sub> solvent at room temperature with tetramethylsilane (TMS) as internal standards. A multiwave ultrasonic generator (Sonicator 3200; Bandelin, MS 73, Germany), equipped with a converter/transducer and titanium oscillator (horn), 12.5 mm in diameter, operating at 20 kHz with a maximum power output of 200 W, was used for the ultrasonic irradiation. The crystallographic structure of prepared catalyst was investigated on a Philips instrument with 1.54 Å wavelengths of X-ray beam and Cu anode material, at a scanning speed of 2° min<sup>-1</sup> from 10° to 80° (2θ). Scanning electron microscope (SEM) of nanoparticles and catalysts were recorded on a FESEM Hitachi S4160. Thermo gravimetric analysis (TGA) was performed on a mettler TA4000 system TG-50 at a heating rate of 10 K min<sup>-1</sup> under N<sub>2</sub> atmosphere. Also, elemental analyses of the catalyst with inductively coupled plasma atomic emission spectroscopy were obtained from an ICP-AES simultaneous instrument (VISTA-PRO). Melting points was obtained with a Yanagimoto micro

melting point apparatus and are uncorrected. The purity determination of the substrates and reaction monitoring were accomplished by TLC on silica-gel polygram SILG/UV 254 plates (from Merck Company).

### 2.2 | Catalyst preparation

New NiFe<sub>2</sub>O<sub>4</sub>@TASDA-Pd(0) complex was prepared based on the following procedure.

### 2.3 | General procedure for preparation of NiFe<sub>2</sub>O<sub>4</sub> nanoparticles

Nickel ferrite nanoparticles (NiFe<sub>2</sub>O<sub>4</sub>) were synthesized by using co-precipitation method, according to the procedure reported in the literature.<sup>[28]</sup> 3 M solution of sodium hydroxide was added drop wise to salt solutions of 0.4 M ferric chloride (FeCl<sub>3</sub> · 6H<sub>2</sub>O) and 0.2 M nickel chloride (NiCl<sub>2</sub> · 6H<sub>2</sub>O). The pH of the solution was constantly monitored as the NaOH solution was added slowly. The reactants were stirred using a magnetic stirrer till pH of the solution was close to 13. Finally 3 drops of oleic acid were added to the solution as a surfactant. The liquid precipitate was then brought to a reaction temperature of 80 °C and stirred for 40 min. The solutions were centrifuged and precipitation was washed several times with double distilled water and ethanol to remove unwanted impurities and the excess surfactant from the synthesized sample. The sample was centrifuged for 15 min at 2000 rpm and then dried overnight at above 80 °C. The acquired substance was then grinded into a fine powder and then calcined for 10 hr at 600 °C. FT-IR (KBr pellets, cm<sup>-1</sup>): 597 (Fe-O) and 421 (Ni-O).

### 2.4 | General procedure for preparation of nano-NiFe<sub>2</sub>O<sub>4</sub>@SiO<sub>2</sub> core-shell

The core-shell NiFe<sub>2</sub>O<sub>4</sub>@SiO<sub>2</sub> nanoparticles were obtained by a Stober method with minor modifications.<sup>[29]</sup> Generally, 100 ml of 75% ethanol/water solution containing the above obtained NiFe<sub>2</sub>O<sub>4</sub> MNPs were transferred into a three-neck flask. After ultrasonic mixing for 10 min, under the condition of N<sub>2</sub> atmosphere, 4 ml of tetraethoxysilane (TEOS) and 2 ml of ammonia were added into NiFe<sub>2</sub>O<sub>4</sub> MNPs suspension in turn under vigorous stirring. The reaction system was kept at 35 °C for 6 hr. Consequently, the black precipitates were NiFe<sub>2</sub>O<sub>4</sub>@SiO<sub>2</sub> MNPs, and were washed with deionized water and ethanol for 3 times and dried at 80 °C for 10 h. FT-IR (KBr pellets, cm<sup>-1</sup>): 3426 (O-H), 1091 (Si-O-Si), 601 (Fe-O) and 469 (Ni-O).<sup>[30]</sup>

## 2.5 | General procedure for functionalization of NiFe<sub>2</sub>O<sub>4</sub>@SiO<sub>2</sub> MNPs surfaces

To our knowledge, the surface of silica nanoparticles can be easily functionalized through aminopropyltriethoxysilane. With vigorously stirring, 400  $\mu$ L of APTES and 600  $\mu$ L of ammonia were added slowly to 50 mL of NiFe<sub>2</sub>O<sub>4</sub>@SiO<sub>2</sub> MNPs solution suspended in 95% ethanol/water solution. The solution was refluxed for 24 hr under an inert atmosphere, separated by an external magnet and washed subsequently with toluene, dichloromethane, and methanol, and dried under reduced pressure at 80 °C for 10 hr to obtain 1.<sup>[31]</sup>

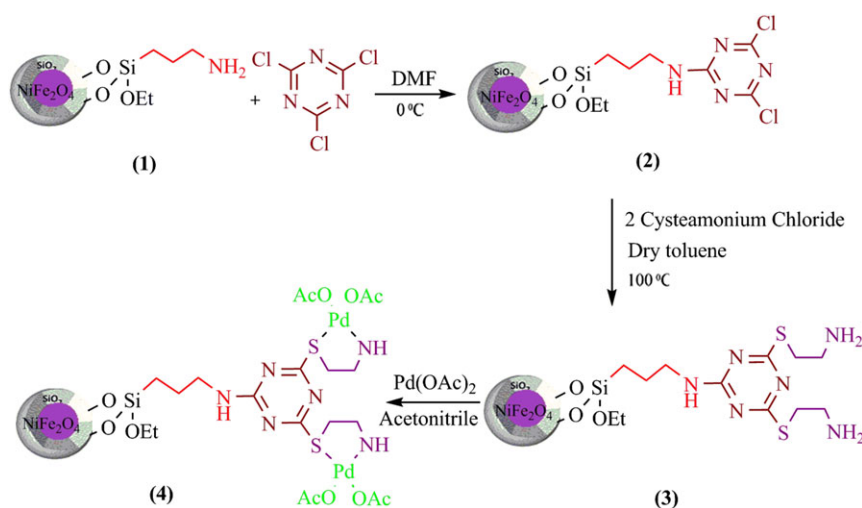
## 2.6 | General procedure for the catalyst NiFe<sub>2</sub>O<sub>4</sub>@TASDA-Pd(0) (4)

For synthesis of ligand 3, to a mixture of 1 (0.50 g) in dry toluene (30 mL) at 0 °C, 1, 3, 5-trichlorotriazine (TCT) (2 mmol, 0.37 g) and diisopropylethyl amine (2 mmol, 0.34 mL) were added and the mixture was stirred at 0 °C for 3 hr. In continue after consumption of TCT and producing of 2, Cysteamonium Chloride (4 mmol, 0.45 g) and diisopropylethyl amine (4 mmol, 0.68 mL) were added slowly to this mixture and refluxed in dry toluene for 24 hr. The residue was separated from the mixture by an external magnet, washed with CH<sub>2</sub>Cl<sub>2</sub> for several times and dried at 80 °C to obtain 3. The final catalyst nanoparticles were prepared as brown solids by addition of Pd (OAc)<sub>2</sub> (10 mg, 0.45 mmol) to a dispersed mixture of 3 in acetonitrile (5 mL) under nitrogen atmosphere at room temperature. Then, the mixture was stirred for 6 hr at 60 °C and next allowed to proceed for an additional 45 min at 70 °C. The final complex was collected

by an external magnet and washed repeatedly with ethanol to remove the unreacted Pd (OAc)<sub>2</sub>, and then dried under air to obtain 4 (Scheme 1). 10 mL NaBH<sub>4</sub> solution (1 mmol) was added to the above solution with mechanically stirring stirred at room temperature for 24 hours. Then, the catalyst was separated from the mixture by an external magnet, washed several times with methanol to remove unreacted Pd (OAc)<sub>2</sub> and dried under vacuum to obtain a black solid powder (5).

## 2.7 | General procedure for the Mizoroki-heck cross-coupling reaction

A mixture of selected aryl halide (1 mmol), styrene (1.2 mmol) and triethylamine (2 mmol) in the presence of 0.002 g Pd complex 4 was added to N,N-dimethylformamide as solvent and the reaction mixture was irradiated in ultrasonic apparatus with the power 45 Watt for 5–17 min according to Table 4. The progress of the reaction was monitored by thin layer chromatography (petroleum ether/ethyl acetate, 5:1). After completion of the reaction, the catalyst was separated by an external magnet, washed with absolute ethanol, dried, and used for the next reactions without further purification. After separation of the catalyst, CH<sub>2</sub>Cl<sub>2</sub> (15 mL) was added and the organic phase was washed with water (3  $\times$  10 mL), and dried over anhydrous MgSO<sub>4</sub>. The resulting solution was evaporated under vacuum to give the crude product. The column chromatography of the crude product on silica gel using n-hexane or different mixtures of n-hexane, ethyl acetate as the eluents afforded the highly pure product (Table 4). The obtained pure products were characterized by spectroscopic data and melting points.



**SCHEME 1** Synthesis of the catalyst NiFe<sub>2</sub>O<sub>4</sub>@TABMA-Pd(0) (5)

## 2.8 | Spectral data for trans-stilbene derivatives

Trans-stilbene; Colorless solid; m.p = 120–122 °C (Lit.<sup>[32]</sup> 125 °C). IR (KBr)/ $\nu$  (cm<sup>-1</sup>): 2992, 1602, 1495, 780. <sup>1</sup>H NMR (400 MHz, CDCl<sub>3</sub>)  $\delta$ : 7.55 (d,  $J$  = 7.6 Hz, 2H), 7.39 (t,  $J$  = 7.6 Hz, 2H), 7.30 (d,  $J$  = 7.2 Hz, 1H), 7.15 (s, 1H).

4-Methoxy-trans-stilbene; Colorless solid; m.p = 130–132 °C (Lit.<sup>[33]</sup> 134–136 °C). IR (KBr)/ $\nu$  (cm<sup>-1</sup>): 3009, 2835, 1606, 1513, 1445, 1368, 1291, 1182. <sup>1</sup>H NMR (400 MHz, CDCl<sub>3</sub>)  $\delta$ : 7.49 (d,  $J$  = 8.8 Hz, 2H), 7.38 (d,  $J$  = 8.0 Hz, 2H), 7.31–7.28 (2H, m), 7.15–7.12 (1H, m), 7.1 (d,  $J$  = 16.4 Hz, 1H), 7.0 (d,  $J$  = 16.4 Hz, 1H), 6.93 (d,  $J$  = 7.2 Hz, 2H), 3.85 (3H, s).

4-Methyl-trans-stilbene; Colorless solid; m.p = 118–120 °C (Lit.<sup>[34]</sup> 119–122 °C). IR (KBr)/ $\nu$  (cm<sup>-1</sup>): 2987, 1600, 1495, 1380, 885. <sup>1</sup>H NMR (400 MHz, CDCl<sub>3</sub>)  $\delta$ : 7.53 (d,  $J$  = 6.8 Hz, 2H), 7.48 (d,  $J$  = 7.6 Hz, 2H), 7.41 (t,  $J$  = 7.6 Hz, 2H), 7.26–7.23 (1H, m), 7.18 (d,  $J$  = 6.8 Hz, 2H), 7.12 (d,  $J$  = 16.6 Hz, 1H), 7.08 (d,  $J$  = 16.6 Hz, 1H), 2.55 (3H, s).

4-nitro-trans-stilbene; Yellow solid; m.p = 156–157 °C (Lit.<sup>[35]</sup> 151–153 °C). IR (KBr)/ $\nu$  (cm<sup>-1</sup>): 3022, 2935, 2837, 1686, 1594, 1574, 1494, 1448, 1338, 1158, 1103, 1078, 983, 972, 851, 773, 692. <sup>1</sup>H NMR (400 MHz, CDCl<sub>3</sub>)  $\delta$ : 8.25 (d,  $J$  = 8.4 Hz, 2H), 7.65 (d,  $J$  = 8.4 Hz, 2H), 7.57 (d,  $J$  = 7.5 Hz, 2H), 7.42–7.36 (m, 3H), 7.30 (d,  $J$  = 16 Hz, 1H), 7.14 (d,  $J$  = 16 Hz, 1H).

3-methyl-trans-stilbene; White solid; m.p = 41–43 °C (Lit.<sup>[36]</sup> 40–45 °C). IR (KBr)/ $\nu$  (cm<sup>-1</sup>): 3023, 1599, 1495, 1448, 965, 782, 748, 692. <sup>1</sup>H NMR (400 MHz, CDCl<sub>3</sub>)  $\delta$ : 7.57 (d,  $J$  = 7.6 Hz, 2H), 7.43–7.38 (d of d,  $J$  = 14.4 Hz, 4H), 7.31 (t,  $J$  = 7.8 Hz, 2H), 7.17 (d,  $J$  = 6.4 Hz, 3H), 2.35 (s, 3H).

4-Cyano-trans-stilbene; Yellow solid; m.p = 115–117 °C (Lit.<sup>[34]</sup> 116–118 °C). IR (KBr)/ $\nu$  (cm<sup>-1</sup>): 3021, 2836, 2361, 1605, 1505, 1363. <sup>1</sup>H NMR (400 MHz, CDCl<sub>3</sub>)  $\delta$ : 7.72–7.53 (m, 5H), 7.46–7.30 (m, 4H), 7.22 (d,  $J$  = 16.4, 1H), 7.09 (d,  $J$  = 16.4, 1H).

4-Acetyl-trans-stilbene; White solid, m.p = 134–136 °C (Lit.<sup>[37]</sup> 135–137 °C). IR (KBr)/ $\nu$  (cm<sup>-1</sup>): 2994, 1680, 1601, 1495, 1383, 880. <sup>1</sup>H NMR (400 MHz, CDCl<sub>3</sub>)  $\delta$ : 7.96 (d,  $J$  = 8.0 Hz, 2H), 7.60 (d,  $J$  = 8.0 Hz, 2H), 7.55 (d,  $J$  = 7.6 Hz, 2H), 7.41 (t,  $J$  = 7.6 Hz, 2H), 7.31 (t,  $J$  = 7.6 Hz, 1H), 7.25 (d,  $J$  = 16.4 Hz, 1H), 7.14 (d,  $J$  = 16.4 Hz, 1H), 2.62 (s, 3H).

2-Styryl-naphthalene; colorless solid; m.p = 50–62 °C (Lit.<sup>[38]</sup> 58–60 °C). IR (KBr)/ $\nu$  (cm<sup>-1</sup>): 3045, 1593. <sup>1</sup>H NMR (400 MHz, CDCl<sub>3</sub>):  $\delta$  = 8.25 (d,  $J$  = 16 Hz, 1H), 8.18 (d,  $J$  = 6.4 Hz, 1H), 8.04 (d,  $J$  = 7.2 Hz, 1H), 7.99 (d,  $J$  = 8 Hz, 1H), 7.69 (t,  $J$  = 8.4 Hz, 2H), 7.83–7.75 (m, 3H), 7.72 (t,  $J$  = 7.2 Hz, m, 2H), 7.65 (t,  $J$  = 7.2 Hz, 1H), 7.44 (d,  $J$  = 15.2 Hz, 1H).

4-Formyl-trans-stilbene; yellow solid; m.p = 118–120 °C (Lit.<sup>[39]</sup> 115–116 °C). IR (KBr)/ $\nu$  (cm<sup>-1</sup>): 2995, 2851, 1701, 1603, 1499, 910, 845. <sup>1</sup>H NMR (400 MHz, CDCl<sub>3</sub>)  $\delta$ : 9.99 (s, 1H), 7.86 (d,  $J$  = 7.6 Hz, 2H), 7.64 (d,  $J$  = 7.6 Hz, 2H), 7.55 (d,  $J$  = 7.6 Hz, 2H), 7.40 (t,  $J$  = 6.0 Hz, 2H), 7.29 (t,  $J$  = 6.4 Hz, 1H), 7.21 (d,  $J$  = 16.4 Hz, 1H), 7.07 (d,  $J$  = 16 Hz, 1H).

1, 4-Bis [(E)-2-phenylethenyl] benzene; light green solid; m.p = 254–258 °C (Lit.<sup>[40]</sup> 254 °C) IR (KBr)/ $\nu$  (cm<sup>-1</sup>): 3024, 1595, 1561, 1510, 1484, 1446, 968. <sup>1</sup>H NMR (400 MHz, CDCl<sub>3</sub>)  $\delta$ : 7.52 (d,  $J$  = 8.4, 2H), 7.45 (d,  $J$  = 7.6, 1H), 7.36 (m, 2H), 7.28 (d,  $J$  = 15.6, 2H), 7.23 (d,  $J$  = 7.6, 1H), 7.14 (m, 1H).

3-chloro-trans-stilbene; white solid; 62–64 °C (Lit.<sup>[38]</sup> 64–69 °C). IR (KBr)/ $\nu$  (cm<sup>-1</sup>): 3045, 2950, 1589. <sup>1</sup>H NMR (400 MHz, CDCl<sub>3</sub>)  $\delta$ : 52 (m, 3H), 7.36 (m, 3H), 7.27 (m, 2H), 7.13 (m, 1H), 7.08 (d,  $J$  = 16 Hz, 1H), 7.01 (d,  $J$  = 16 Hz, 1H).

Methyl (E)-4-styryl benzoate; white solid, m.p = 154–156 °C (Lit.<sup>[41]</sup> 158 °C). IR (KBr)/ $\nu$  (cm<sup>-1</sup>): 3024, 2945, 1708, 1602, 1434, 1277, 1179, 1105, 963, 835, 771, 698, 670, 579. <sup>1</sup>H NMR (400 MHz, CDCl<sub>3</sub>)  $\delta$ : 8.03 (d,  $J$  = 6.7 Hz, 2H), 7.50–7.58 (m, 4H), 7.46–7.32 (m, 3H), 7.28 (d,  $J$  = 16 Hz, 1H), 7.13 (d,  $J$  = 16 Hz, 1H), 3.93 (s, 3H). The FT-IR and <sup>1</sup>H NMR spectra of all compounds are included in the Supplementary information.

## 3 | RESULT AND DISCUSSION

Nickel ferrite nanoparticles were synthesized by using co-precipitation method, according to the procedure reported in the literature.<sup>[33]</sup> The synthetic pathway for preparation of the catalyst is shown in Scheme 1. In order to characterize the catalyst structure, the synthesized nano catalyst was analyzed using X-ray diffraction (XRD), Fourier transform infrared (FT-IR) spectra, scanning electron microscopy (SEM), energy-dispersive X-ray spectroscopy (EDX), vibrating sample magnetometer (VSM), and also, thermo-gravimetric analysis (TGA) techniques.

### 3.1 | Characterization results of NiFe<sub>2</sub>O<sub>4</sub>@TASDA-Pd(0)

Figure 1 shows the FT-IR spectrum of NiFe<sub>2</sub>O<sub>4</sub> NPs, NiFe<sub>2</sub>O<sub>4</sub>@SiO<sub>2</sub>, NiFe<sub>2</sub>O<sub>4</sub>@SiO<sub>2</sub>-NH<sub>2</sub> NPs, NiFe<sub>2</sub>O<sub>4</sub>@TASDA-Pd(0) before reaction and NiFe<sub>2</sub>O<sub>4</sub>@TASDA-Pd(0) after reaction in the range 400–4000 cm<sup>-1</sup>. The bands at 3415 and 1620 cm<sup>-1</sup> can be assigned to the stretching modes of absorbed water. The band at 597 cm<sup>-1</sup> is attributed to the vibration of Fe—O bonds. The characteristic band at 421 cm<sup>-1</sup> can be assigned to



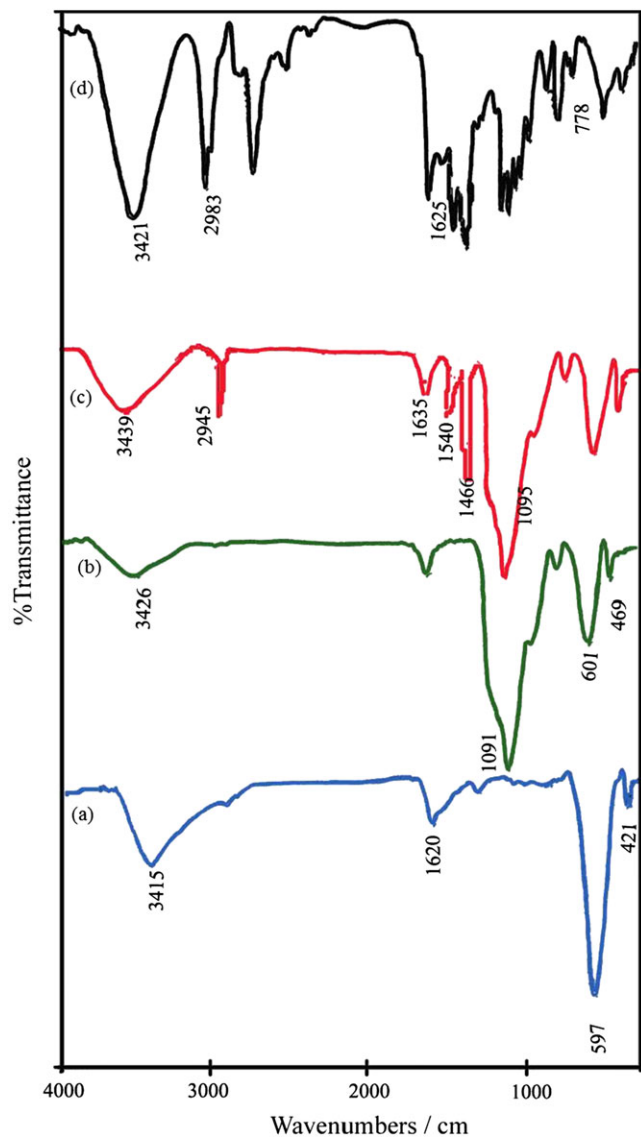


**FIGURE 1** FT-IR spectrum of a)  $\text{NiFe}_2\text{O}_4$  NPs, b)  $\text{NiFe}_2\text{O}_4@\text{SiO}_2$ , c)  $\text{NiFe}_2\text{O}_4@\text{SiO}_2\text{-NH}_2$  NPs and d)  $\text{NiFe}_2\text{O}_4@\text{TASDA}$  before reaction, e)  $\text{NiFe}_2\text{O}_4@\text{TASDA}$  after reaction

metal vibrations of Ni—O bonds (Figure 1a). In all three spectra (Figure 1a, 1b, 1c), the revealed peaks of  $\text{NiFe}_2\text{O}_4$  were observed at  $421\text{--}601\text{ cm}^{-1}$ , which could be attributed to the characteristic absorption of Fe—O and Ni—O bond. In  $\text{NiFe}_2\text{O}_4@\text{SiO}_2$  spectrum (Figure 1b),  $\text{NiFe}_2\text{O}_4@\text{SiO}_2\text{-NH}_2$  spectrum (Figure 1c), final catalyst spectrum (Figure 1d), and  $\text{NiFe}_2\text{O}_4@\text{TASDA}$  after five recycles (Figure 1e), the intense peak at  $1091, 1095, 1096, 1096\text{ cm}^{-1}$  was derived from the Si—O—Si stretching vibrations. These peaks proved that  $\text{SiO}_2$  has coated the surface of  $\text{NiFe}_2\text{O}_4$ . In  $\text{NiFe}_2\text{O}_4@\text{SiO}_2\text{-NH}_2$  spectrum, the characterized peaks at  $1635, 1540\text{ cm}^{-1}$  could be attributed to the C—N stretching vibrations and  $\text{NH}_2$  bending vibration. Moreover, the peak at  $2945\text{ cm}^{-1}$  is related to stretching vibration of  $\text{CH}_2$ , the peak at  $1466\text{ cm}^{-1}$  is related to bending vibration of  $\text{CH}_2$  and the peak at  $3439\text{ cm}^{-1}$  is assigned to the N—H stretching vibration. These described peaks confirmed that  $\text{NiFe}_2\text{O}_4@\text{SiO}_2\text{-NH}_2$  NPs are prepared. The FT-IR spectrum of  $\text{NiFe}_2\text{O}_4@\text{TASDA}$  absorption bands at  $1625\text{ cm}^{-1}$  (C=N),  $2983\text{ cm}^{-1}$  (C—H),  $3421\text{ cm}^{-1}$  (N—H stretching vibration) and  $778\text{ cm}^{-1}$  (C—S stretching vibration). The Figure 1 e shows the FT-IR spectrum of  $\text{NiFe}_2\text{O}_4@\text{TASDA-Pd(0)}$  after five recycles. We did not observe significant change in the FT-IR spectrum of the catalysts after five repeated reaction.

The powder XRD pattern of the nickel ferrite nanoparticles is shown in Figure 2a. All of the characteristics peaks of  $\text{NiFe}_2\text{O}_4$  are present in the diffraction pattern and the diffraction peaks match with standard XRD pattern (JCPDS file no. 03–0875). The sizes of the nanoparticles are determined as around 30 nm from the Scherrer equation using the peak broadening of the most intense peak. Figure 2b shows the appearance of new peaks at  $2\theta = 39.7^\circ, 46.3^\circ$ , and  $67.5^\circ$  attributed to Pd species. The results indicate that the Pd have been successfully immobilized on  $\text{NiFe}_2\text{O}_4$  particle surfaces.

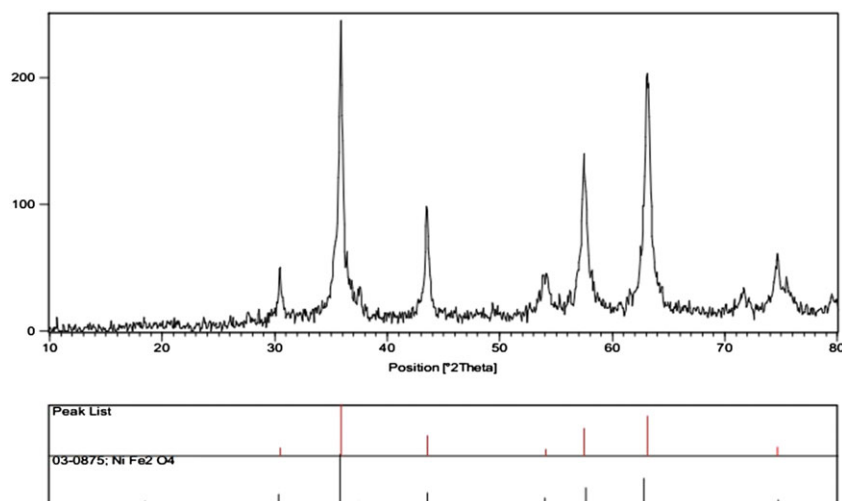


**FIGURE 2** The X-ray diffraction patterns of a) calcinated  $\text{NiFe}_2\text{O}_4$ , b)  $\text{NiFe}_2\text{O}_4@\text{TABMA-Pd(0)}$

Figure 3 shows the SEM image of  $\text{NiFe}_2\text{O}_4$  and final catalyst, in that the spherical morphology with an average diameter of about 50 nm for  $\text{NiFe}_2\text{O}_4$  and 60 nm for catalyst was observed. Elemental analysis was also performed. Figure 4 shows the EDX spectra of  $\text{NiFe}_2\text{O}_4$  and final catalyst. The elemental analysis of  $\text{NiFe}_2\text{O}_4$  NPs indicated that the amounts of oxygen, iron and nickel were about 54.55, 37.05, and 8.40%, respectively. The

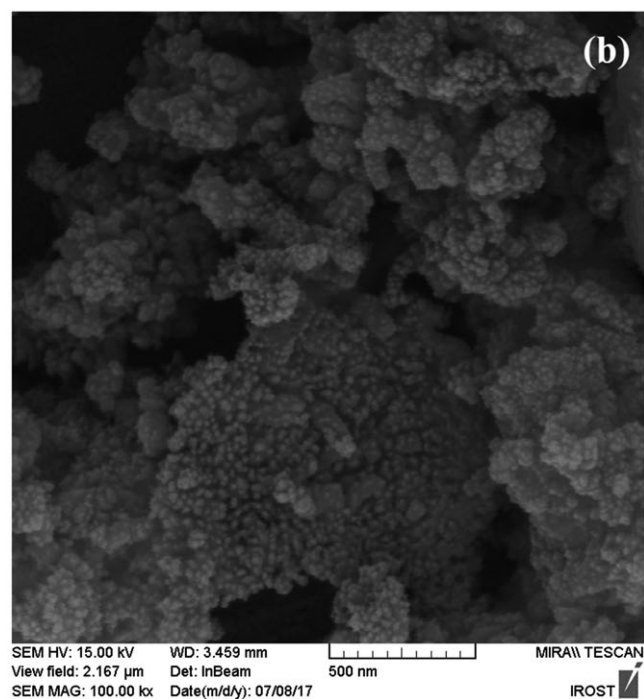
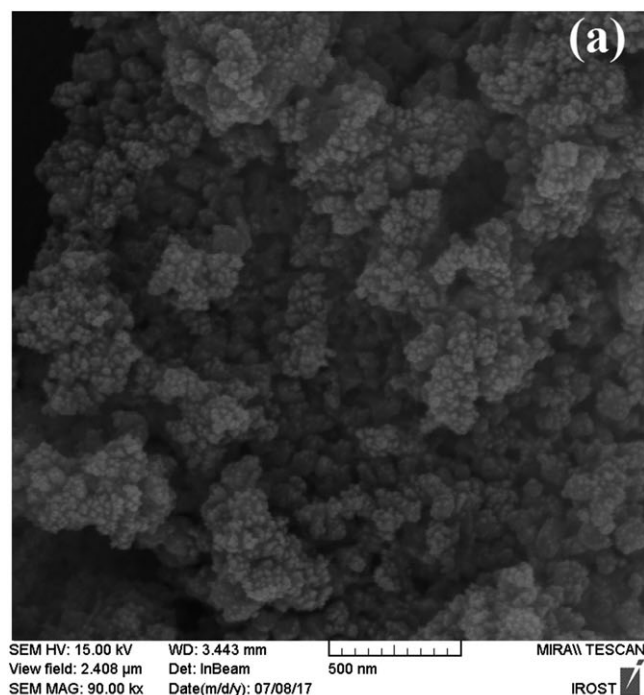


**FIGURE 3** SEM images of  $\text{NiFe}_2\text{O}_4$  nanoparticles (a)  $\text{NiFe}_2\text{O}_4$  (b)  $\text{NiFe}_2\text{O}_4$ @TASDA-Pd(0)

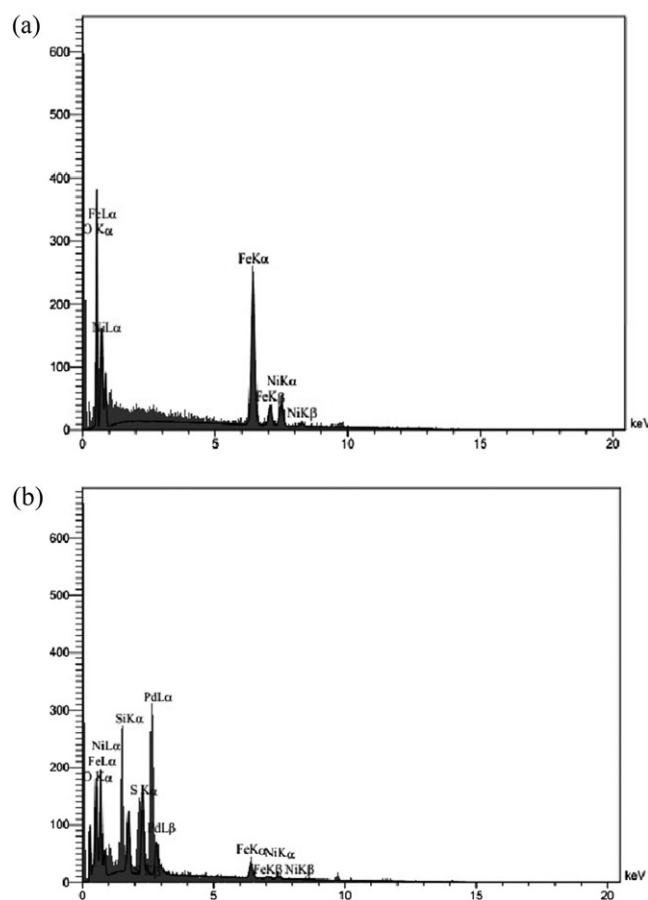


**FIGURE 4** (a) EDX spectrum of the  $\text{NiFe}_2\text{O}_4$  nanoparticles. (b) EDX spectrum of the  $\text{NiFe}_2\text{O}_4$ @TASDA-Pd(0)

results showed the presence of C, N, O, Si, S, Fe, Ni and Pd in the composites, which confirmed that the catalyst has been successfully synthesized. Also, to support the mentioned observation, the catalyst was subjected to inductively coupled plasma (ICP) analyzer. ICP analysis indicated the presence of Pd in the catalyst and the content of Pd was estimated to be  $0.17 \text{ mmol g}^{-1}$  (18.4%W).

Thermal stability of the synthesized catalyst was investigated by TGA and the related curves are demonstrated in Figure 5. Herein TGA analysis curves of  $\text{NiFe}_2\text{O}_4$ @ $\text{SiO}_2$  and final catalyst are compared. Both curves illustrate similar characteristics. As demonstrated in Figure 5a, 6% decrease in weight before  $150^\circ\text{C}$  is attributed to the removal of surface hydroxyl groups and physically adsorbed solvent and water molecules trapped in  $\text{SiO}_2$  layer. The weight loss 7% between  $400$  and  $600^\circ\text{C}$  is attributed to the decomposition of less stable functional groups for example hydroxyl grafted to the silica surface. As illustrated in Figure 5b, a little weight loss (10%) between  $150^\circ\text{C}$  and  $250^\circ\text{C}$  is attributed to the trapped water. While the organic components (40%) was lost between  $250$  and  $400^\circ\text{C}$ . These results show that catalyst is stable up to  $250^\circ\text{C}$  and can be used in organic synthesis.

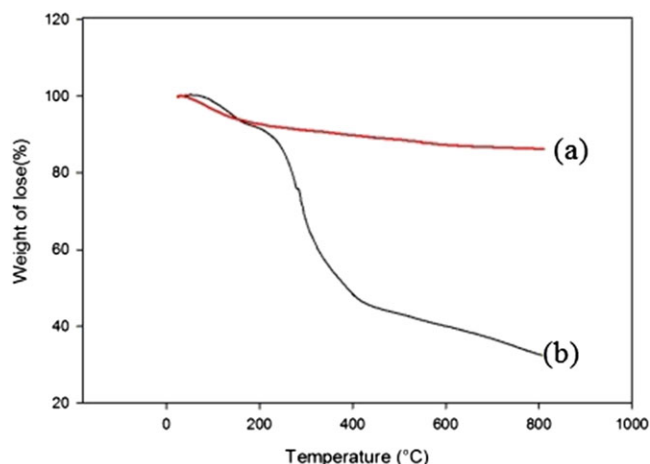


**FIGURE 5** Thermo gravimetric analysis of a)  $\text{NiFe}_2\text{O}_4@\text{SiO}_2$  b)  $\text{NiFe}_2\text{O}_4@\text{TASDA-Pd(0)}$

Magnetic properties of  $\text{NiFe}_2\text{O}_4$  nanoparticles and final catalyst were investigated with VSM at room temperature (Figure 6). Magnetization of samples could be completely saturated at high fields of up to 1.0 T and the saturation magnetization of samples decreased from 35 to  $3.5 \text{ emu g}^{-1}$ , because of the functionalization by extra organic layer. Furthermore, these results illustrate that the magnetization property decreases by coating and functionalization. It is of very importance that a catalyst should possess enough magnetic properties for its experimental application.

### 3.2 | Investigation of catalyst activity

To examine the catalytic performance of the nanocatalyst and to characterize optimal conditions for Mizoroki–Heck coupling reaction, iodobenzene and styrene was selected as model reagents and were investigated under

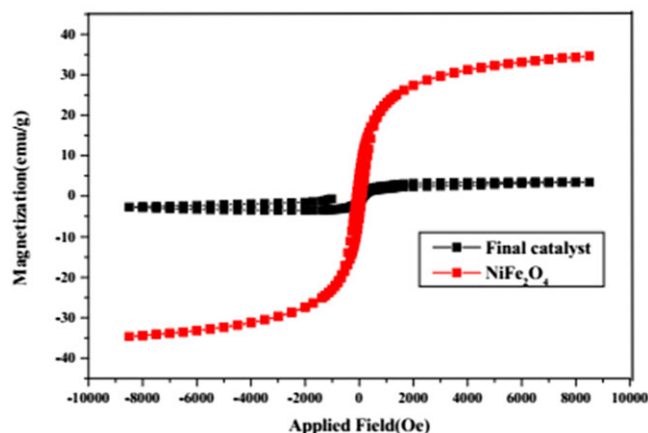


**FIGURE 6** The vibrating sample magnetometer curve of  $\text{NiFe}_2\text{O}_4$  nanoparticles and  $\text{NiFe}_2\text{O}_4@\text{TASDA-Pd(0)}$

different parameters such as solvent, bases, various amounts of catalyst and the effect of ultrasound irradiation.

In our first set of experiments, we examined efficiency of the different solvent in Mizoroki–Heck reaction. Several organic solvents such as acetonitrile, ethanol, dimethylformamide, dimethyl sulfoxide and toluene were examined. According to data given in Table 1, entry 4, DMF was the most efficient solvent for this transformation. Other solvents gave only moderate yields of the product. In the following step, it was obtained the suitable base for the coupling reaction. We studied different bases, among the various bases screened,  $\text{NEt}_3$  was found to be the best base for this reaction (Table 1, entry 9). The other bases such as  $\text{Na}_2\text{CO}_3$  and  $\text{K}_2\text{CO}_3$  gave moderate yields of the product.

In continuation of this research, the activity of the catalyst in different amounts on the reaction was investigated. No reaction was observed in the absence of catalyst under ultrasonic irradiation (Table 2, entry 1). The results demonstrated that in the presence of ultrasonic irradiation and 0.02 g of the  $\text{NiFe}_2\text{O}_4@\text{TASDA-Pd(0)}$  catalyst, the reaction time is decreased to 8 min and the yield increased sharply to 99% (Table 2, entry 5).

In next step, power of the ultrasonic irradiation was optimized. The model reaction was performed in the presence of 0.020 g of  $\text{NiFe}_2\text{O}_4@\text{TASDA-Pd(0)}$  catalyst in DMF under silent condition and various powers of ultrasound irradiation to investigate the best operating

**TABLE 1** Optimization in the presence of different solvents and bases<sup>a</sup>

| Entry | Solvent                | Base                    | Yield <sup>b</sup> |
|-------|------------------------|-------------------------|--------------------|
| 1     | EtOH                   | $\text{K}_2\text{CO}_3$ | 75                 |
| 2     | $\text{CH}_3\text{CN}$ | $\text{K}_2\text{CO}_3$ | 81                 |
| 3     | DMSO                   | $\text{K}_2\text{CO}_3$ | 68                 |
| 4     | DMF                    | $\text{K}_2\text{CO}_3$ | 91                 |
| 5     | Toluene                | $\text{K}_2\text{CO}_3$ | 35                 |
| 6     | DMF                    | KOH                     | 55                 |
| 7     | DMF                    | $\text{NaHCO}_3$        | 46                 |
| 8     | DMF                    | $\text{K}_3\text{PO}_4$ | 78                 |
| 9     | DMF                    | $\text{NEt}_3$          | 99                 |

<sup>a</sup>Reaction conditions: Iodobenzene (1 mmol), styrene (1.2 mmol), amount of catalyst (30 mg), Power (50 w) time (30 min), base (2 mmol), solvent (5 ml).

<sup>b</sup>Isolated yield.

**TABLE 2** Optimization of the various amount of catalyst<sup>a</sup>

| Entry | Conditions | Pd catalyst | Time (min) | Yield <sup>b</sup> (%) |
|-------|------------|-------------|------------|------------------------|
| 1     | US         | 0           | 30         | 0                      |
| 2     | US         | 0.005       | 20         | 72                     |
| 3     | US         | 0.010       | 16         | 84                     |
| 4     | US         | 0.015       | 13         | 91                     |
| 5     | US         | 0.020       | 8          | 99                     |
| 6     | US         | 0.025       | 8          | 99                     |

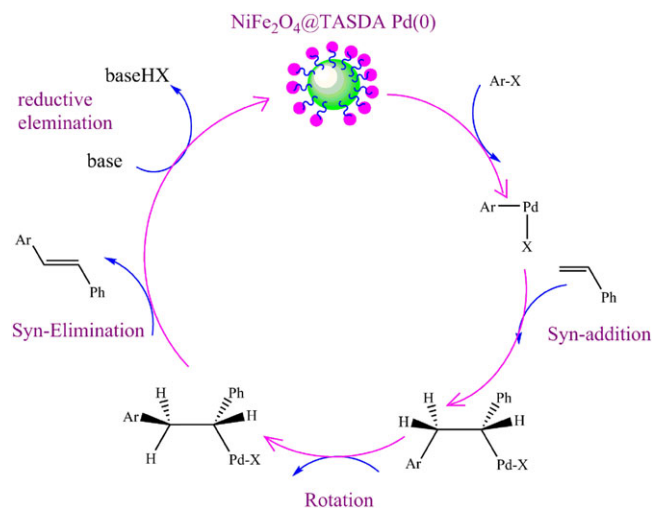
<sup>a</sup>Reaction conditions: Iodobenzene (1 mmol), styrene (1.2 mmol), Power (50 w) and NEt<sub>3</sub> (2 mmol) in DMF.

<sup>b</sup>Isolated yield.

suitable power of ultrasonic irradiation. The effective power was found to be 45 watt (Table 3, entry 5).

After optimization of the reaction conditions, a broad range of structurally diverse aryl halides were reacted with styrene in the presence of 20 mg of NiFe<sub>2</sub>O<sub>4</sub>@TASDA-Pd(0) catalyst and 2 mmol triethylamine with DMF as solvent under ultrasonic irradiation at room temperature (Scheme 2), and the results are displayed in Table 4. To assess the effect of sonication on this reaction, we initially investigated this reaction under thermal conditions (Table 4). As displayed in Table 4, the reaction performs efficiently in high yield between 2.5–12 hours at 130 °C. As shown in Table 4, in the presence of Pd nanocatalyst, excellent product yields were achieved in shorter reaction time under ultrasound irradiation.

Ultrasonic irradiation differs from conventional energy sources. We think that the main effect of ultrasound on this transformation perhaps related to a better mass transfer and dispersion of the catalyst in the medium in comparison with traditional methods, which makes the catalyst very active in this reaction. Ultrasound advances the chemical reactions in a solution through the production of cavitations micro bubbles. The sudden implosion of these micro bubbles in the solutions produces localized

**SCHEME 2** Cross-coupling of aryl halides and styrene

hot spots with very short life cycle. The high local temperature and pressures provide favorable conditions for advancing a large number of organic reactions. Therefore, the ultrasound can be increased the rate of reaction and therefore decreased the energy consumption. The chemical and physical effects of ultrasound are based on acoustic cavitations, which include formation, growth and collapse of bubbles in a solution, which results in a high temperature and pressure pulse and due to increase in the reactant impact surface area through cavitations event. The advantages of sonication on organic reactions are the formation of purer products in excellent yields, very short reaction times, waste minimization and mild conditions which is comparable to traditional methods.

In order to illustrate the merit of this proposed research, we compared the obtained results with the recently reported results. For this purpose, the reactions of iodobenzene and styrene using 20 mg of catalyst in DMF under ultrasonic irradiation in the presence of 2 mmol NEt<sub>3</sub> were chosen as model reaction and the comparison was performed on the basis of reaction conditions, reaction time and obtained yields (Table 5, entry 1 vs. other entries). The advantages of this research which make it exclusiveness than other previously reported procedures, are mild reaction condition, environmentally benign, simple recycle of the nano catalyst by an external magnet, reusability of the catalyst for five times without considerable loss of catalytic activity, excellent yield of trans-stilbene and short reaction time. However, the phosphine ligands have been applied to stabilize active palladium intermediates, for Pd-catalysed carbon-carbon coupling reactions. While, the oxygen and water sensitivity, expensive, toxicity and unrecoverable of these classes of ligands, prevents their usage in a diversity of synthetic applications.

**TABLE 3** Study of the effect of ultrasonic irradiation on the Mizoroki-Heck cross-coupling<sup>a</sup>

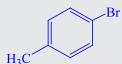
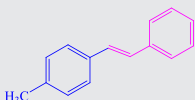
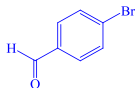
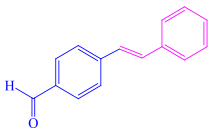
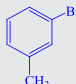
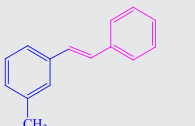
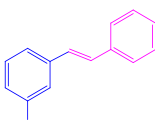
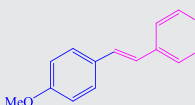
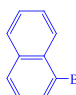
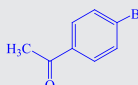
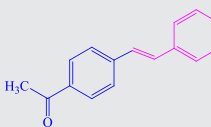
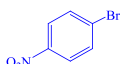
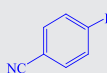
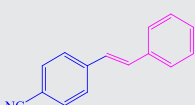
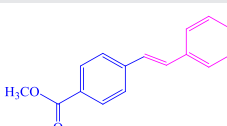
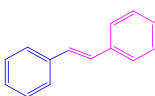
| Entry | Power (w) | Time (min) | Yield (%) <sup>b</sup> |
|-------|-----------|------------|------------------------|
| 1     | 25        | 30         | 61                     |
| 2     | 30        | 26         | 73                     |
| 3     | 35        | 21         | 85                     |
| 4     | 40        | 15         | 91                     |
| 5     | 45        | 8          | 99                     |
| 6     | 50        | 8          | 99                     |

<sup>a</sup>Reaction conditions: Iodobenzene (1 mmol), styrene (1.2 mmol) amount of catalyst (20 mg), and NEt<sub>3</sub> (2 mmol) in DMF.

<sup>b</sup>Isolated yield.

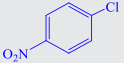
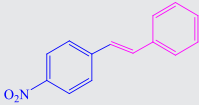
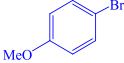
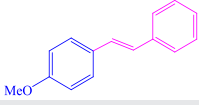
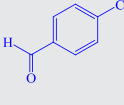
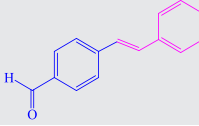
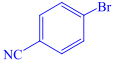
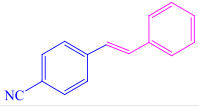
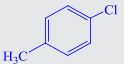
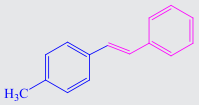


**TABLE 4** Mizoroki–Heck cross-coupling of aryl halides and styrene in the presence of  $\text{NiFe}_2\text{O}_4\text{@TASDA-Pd(0)}^{\text{a}}$ 

| Entry | Aryl halide   | Product   | Thermal conditions <sup>b</sup><br>Time (h) Yield <sup>d</sup> (%) | Ultrasonic conditions <sup>c</sup><br>Time (min) Yield <sup>d</sup> (%) |
|-------|---|---|--|---|
| 1     |    |    | 4/96   | 8/99  |
| 2     |    |    | 5.5/87   | 10/95   |
| 3     |    |    | 6/90   | 12/96   |
| 4     |    |    | 5/81   | 9/94  |
| 5     |    |    | 7/87   | 14/95   |
| 6     |    |    | 3/78   | 6/92  |
| 7     |  |  | 8/72   | 14/92   |
| 8     |  |  | 7/91   | 13/94   |
| 9     |  |  | 6/94   | 12/98   |
| 10    |  |  | 2.5/95   | 5/98  |
| 11    |  |  | 7/80   | 15/93   |
| 12    |  |  | 7/90   | 14/93   |
| 13    |  |  | 7/85   | 12/93   |

(Continues)

TABLE 4 (Continued)

| Entry | Aryl halide   | Product   | Thermal conditions <sup>b</sup><br>Time (h) Yield <sup>d</sup> (%) | Ultrasonic conditions <sup>c</sup><br>Time (min) Yield <sup>d</sup> (%) |
|-------|---|---|--|---|
| 14    |  |  | 10/66  | 25/65   |
| 15    |  |  | 9/83   | 16/87   |
| 16    |  |  | 11/65  | 30/63   |
| 17    |  |  | 8/80   | 13/90   |
| 18    |  |  | 12/51  | 35/58   |

<sup>a</sup>Reaction conditions: Aryl halide (1 mmol), styrene (1.2 mmol, for entry 12, 2.2 mmol), amount of catalyst (0.02 g) and NEt<sub>3</sub> (2 mmol) in DMF.

<sup>b</sup>At 130 °C.

<sup>c</sup>Applied power: 45 W.

<sup>d</sup>Isolated yield.

TABLE 5 Comparison of the results of trans-stilbene synthesis in present method with various reports in the literature

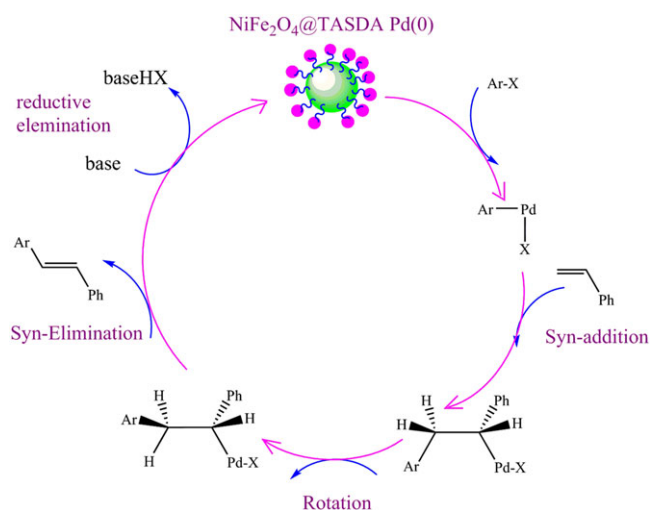
| Entry | Catalyst   | Time (h) | Yield (%) <sup>a</sup> | Ref.      |
|-------|--|----------|------------------------|-----------|
| 1     | NiFe <sub>2</sub> O <sub>4</sub> @TASDA-Pd(0)      | 0.13     | 99                     | This work |
| 2     | Pd/NiFe <sub>2</sub> O <sub>4</sub>                | 2        | 50                     | [42]      |
| 3     | Pd loaded NiFe <sub>2</sub> O <sub>4</sub>         | 4        | 97                     | [43]      |
| 4     | Pd/NiFe <sub>2</sub> O <sub>4</sub> /GO            | 3        | 98                     | [44]      |
| 5     | Si-PNHC-Pd   | 7        | 90                     | [45]      |
| 6     | SPIONs-bis (NHC)-pd (II)                           | 2        | 90                     | [46]      |
| 7     | Pd/MFC   | 2        | 66                     | [47]      |
| 8     | palladium acetate                                  | 2        | 75                     | [4]       |
| 9     | PdCl <sub>2</sub> (SET <sub>2</sub> ) <sub>2</sub> | 23       | 71                     | [48]      |

<sup>a</sup>Isolated yield.

### 3.3 | The proposed reaction mechanism

The pathway of the olefination of halobenzenes with NiFe<sub>2</sub>O<sub>4</sub>@TASDA-Pd(0) catalyst in DMF with NEt<sub>3</sub> is proposed, which is shown in Scheme 2. Initially, oxidative addition of aryl halides to palladium (0) leads to a

palladium (II) species. Then, the alkene coordinates to palladium (II) species, which then undergoes an insertion reaction to form the palladium (II) complex. The coupled aryl and alkenyl compound of the palladium (II) complex is then eliminated via a β-hydride removal followed by reductive elimination with base to retain the original palladium (0) (Scheme 3).



SCHEME 3 The proposed reaction mechanism

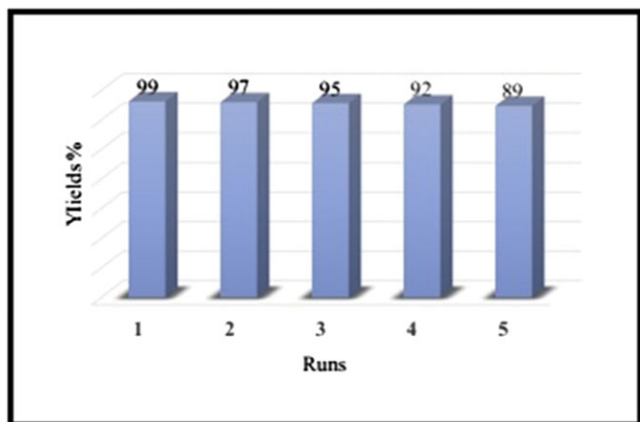


**FIGURE 7** Reusability of catalyst for the synthesis of trans-stilbene derivatives

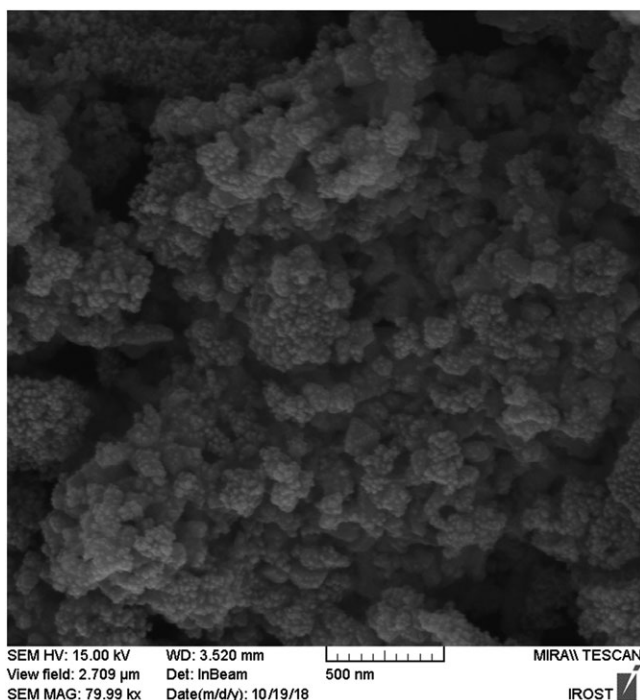


**FIGURE 8** SEM image of  $\text{NiFe}_2\text{O}_4\text{@TASDA-Pd(0)}$  after five recycles

### 3.4 | Catalyst reusability

The recyclability of the  $\text{NiFe}_2\text{O}_4\text{@TASDA-Pd(0)}$  catalyst as a heterogeneous catalyst was investigated in the coupling of iodobenzene and styrene using 20 mg of catalyst in DMF at ultrasonic irradiation in the presence of 2 mmol of  $\text{NEt}_3$ . After the completion of the reaction, the catalytic system was separated from the reaction mixture using an external magnet and the residual catalyst was washed with ethanol several times, dried and reused in subsequent reactions. As can be seen after five cycles, the catalyst was demonstrated approximately the same

activity and led to the corresponding product in high yields (Figure 7). Also the SEM image for the characterization of catalyst after five recycles was shown in Figure 8. After five repeated reaction cycles, it was observed any significant change in the morphology of the catalyst, but some Pd particles might be aggregated onto the surfaces of the matrices.

## 4 | CONCLUSION

In conclusion, we have reported a novel, efficient, mild, fast, clean, and safe sonochemical method for the synthesis of trans-stilbene derivatives by  $\text{NiFe}_2\text{O}_4\text{@TASDA-Pd(0)}$  catalyst at room temperature. We have applied palladium catalyst as a highly active, reusable and recoverable heterogeneous catalyst in the Mizoroki–Heck cross-coupling reactions. This reactions produced the corresponding trans-coupled products stereo selectively in excellent yields and acceptable reaction times. The catalyst can be separated by external magnet and reuse several times without any significant loss of activity which is an additional sustainable characteristic of this method. The products have been confirmed by spectroscopic and physical data such as; IR,  $^1\text{H}$  NMR, and melting point.

## ACKNOWLEDGEMENTS

The authors are grateful to University of Kashan for supporting this work by Grant No. 159148/78.

## ORCID

Hossein Naeimi  <https://orcid.org/0000-0002-9627-596X>

## REFERENCES

- [1] W. A. Herrmann, V. P. W. Bohm, *J. Organometallic. Chem.* **1999**, 572, 141.
- [2] A. Minatti, X. Zheng, S. L. Buchwald, *J. Org. Chem.* **2007**, 72, 9253.
- [3] G. D. Frey, J. Schütz, E. Herdtweck, W. A. Herrmann, *Organometallics* **2005**, 24, 4416.
- [4] R. F. Heck, J. P. Nolley, *J. Org. Chem.* **1972**, 37, 2320.
- [5] L. Djakovitch, H. Heise, K. Köhler, *J. Organometallic. Chem.* **1999**, 584, 16.
- [6] M. Tsutomu, M. Kunio, O. Atsumu, *Bull. Chem. Soc. Jpn.* **1977**, 44, 159.
- [7] I. P. Beletskaya, A. V. Cheprakov, *Chem. Rev.* **2000**, 100, 3009.
- [8] K. Sakod, J. Mihara, J. Ichikawa, *Chem. Commun.* **2005**, 4684.
- [9] L. A. Arnold, W. Luo, R. K. Guy, *Org. Lett.* **2004**, 6, 3005.
- [10] A. B. Dounay, L. E. Overman, A. D. Wroblewski, *J. Am. Chem. Soc.* **2005**, 127, 10186.

- [11] J. Mo, L. Xu, J. Ruan, S. Liua, J. Xiao, *Chem. Commun.* **2006**, 3591.
- [12] T. Tu, X. L. Hou, L. X. Dai, *Org. Lett.* **2003**, 5, 3651.
- [13] B. Mariampillai, C. Herse, M. Lautens, *Org. Lett.* **2005**, 7, 4745.
- [14] A. A. Sabino, A. H. L. Machado, C. R. D. Correia, M. N. Eberlin, *Angew. Chem. Int. Ed.* **2004**, 43, 2514.
- [15] F. Zhao, B. M. Bhanage, M. Shirai, M. Arai, *J. Mol. Catal. A: Chem.* **1999**, 142, 383.
- [16] W. Cabri, I. Candiani, *Chem. Res.* **1995**, 28, 2.
- [17] A. A. Kelkar, T. Hanaoka, Y. Kubota, Y. Sugi, *Catalysis Lett.* **1994**, 29, 69.
- [18] W. A. Herrmann, C. Brossmer, C. P. Reisinger, T. H. Riermeier, K. Ofele, M. Beller, *Chem. – Eur. J.* **1997**, 3, 1357.
- [19] W. A. Herrmann, C. Brossmer, K. Ofele, C. P. Reisinger, T. Priemeier, M. Beller, H. Fischer, *Angew. Chem. Int. Ed.* **1995**, 34, 1844.
- [20] R. S. Varma, K. P. Naicker, P. J. Liesen, *Tetrahedron Lett.* **1999**, 40, 2075.
- [21] M. Seki, T. Seiyaku, *Synth. Commun.* **2006**, 18, 2975.
- [22] H. Lim, M. Chul Cha, J. Young Chang, *Polym. Chem.* **2012**, 3, 868.
- [23] Z. Liu, H. Wang, C. Liu, Y. Jiang, G. Yu, X. Mu, X. Wang, *Chem. Commun.* **2012**, 48, 7350.
- [24] R. Hudson, C. J. Li, A. Moores, *Green Chem.* **2012**, 14, 622.
- [25] W. T. Richards, A. L. Loomis, *J. Am. Chem. Soc.* **1927**, 49, 3086.
- [26] T. J. Mason, *Chem. Soc. Rev.* **1997**, 26, 443.
- [27] M. Nasrollahzadeh, A. Ehsani, A. Rostami-Vartouni, *Ultrason. Sonochem.* **2014**, 21, 275.
- [28] K. Maaz, S. Karim, A. Mumtaz, S. K. Hasanain, J. Liu, J. L. Duan, *J. Magn. Mater.* **2009**, 321, 1838.
- [29] H. Lei, L. Zhiyang, F. Jing, D. Yan, H. Nongyue, W. Zhifei, W. Hua, S. Zhiyang, W. Zunliang, *J. Biomed. Nanotechnol.* **2009**, 5, 596.
- [30] L. Zhiyang, H. Lei, S. Zhiyang, W. Hua, L. Song, L. Hongna, W. Zhifei, H. Nongyue, *J. Biomed. Nanotechnol.* **2009**, 5, 505.
- [31] J. Hongrong, Z. Xin, X. Zhijiang, L. Ming, L. Chuanyan, L. Zhiyang, J. Lian, W. Zhifei, D. Yan, H. Nongyue, *J. Biomed. Nanotechnol.* **2013**, 9, 674.
- [32] X. Cui, Z. Li, C. Z. Tao, Y. Xu, J. Li, L. Liu, Q. X. Guo, *Org. Lett.* **2006**, 8, 2467.
- [33] M. Gozin, A. Weisman, Y. Ben-David, D. Milstein, *Nat. Prod. Lett.* **1993**, 343, 699.
- [34] G. Ren, X. Cui, E. Yang, F. Yang, Y. Wu, *Tetrahedron* **2010**, 66, 4022.
- [35] R. Bandari, T. Hçche, A. Prager, K. Dirnberger, M. R. Buchmeiser, *Chem. – Eur. J.* **2010**, 16, 4650.
- [36] Y. G. Zhang, X. L. Liu, Z. Y. He, X. M. Li, H. J. Kang, S. K. Tian, *Chem. – Eur. J.* **2014**, 20, 2765.
- [37] L. R. Moore, E. C. Western, R. Craciun, J. M. Spruell, D. A. Dixon, K. P. O'Halloran, K. H. Shaughnessy, *Organometallics* **2008**, 27, 576.
- [38] A. R. Hajipour, K. Karami, A. Pirisedigh, A. E. Ruoho, *J. Organomet. Chem.* **2009**, 694, 2548.
- [39] B. R. Baker, R. E. Gibson, *J. Med. Chem.* **1971**, 14315.
- [40] A. Chaieb, A. Khoukh, R. Brown, J. François, C. D. Lartigau, *Opt. Mater.* **2007**, 30, 318.
- [41] K. V. Kutonova, M. E. Trusova, A. V. Stankevich, P. S. Postnikov, V. D. Filimonov, *J. Org. Chem.* **2015**, 11, 358.
- [42] S. R. Borhade, S. B. Waghmode, *J. Org. Chem.* **2010**, 7, 310.
- [43] Z. Gao, Y. Feng, F. Cui, Z. Hua, J. Zhou, Y. Zhu, J. Shi, *J. Mol. Catal. A: Chem.* **2011**, 336, 51.
- [44] X. Liua, X. Zhao, J. Zhu, J. Xu, *Appl. Organometal. Chem.* **2016**, 30, 354.
- [45] B. Tamami, F. Farjadian, S. Ghasemi, H. Allahyari, *New. J. Chem.* **2013**, 3, 7.
- [46] M. Ghotbinejad, A. R. Khosropour, I. Mohammadpoor-Baltork, M. Moghadam, S. Tangestaninejad, V. Mirkhani, *J. Mol. Catal. A: Chem.* **2014**, 385, 78.
- [47] B. Baruwati, D. Guin, S. V. Manorama, *Org. Lett.* **2007**, 9, 5377.
- [48] A. S. Gruber, D. Pozebon, A. L. Monteiro, J. Dupont, *Tetrahedron Lett.* **2001**, 42, 7345.

## SUPPORTING INFORMATION

Additional supporting information may be found online in the Supporting Information section at the end of the article.

**How to cite this article:** Naeimi H, Kiani F. Magnetically thiamine palladium complex nanocomposites as an effective recyclable catalyst for facile sonochemical cross coupling reaction. *Appl Organometal Chem.* 2019;e4742. <https://doi.org/10.1002/aoc.4742>